Molecular Temperature Probes

DOI: 10.1002/anie.201305835

DNA as a Molecular Local Thermal Probe for the Analysis of Magnetic Hyperthermia**

Jorge T. Dias, María Moros, Pablo del Pino, Sara Rivera, Valeria Grazú, and Jesus M. de la Fuente**

The magnetism of magnetic nanoparticles (MNPs)[1] has found many useful applications in nanomedicine. Among them, heating with MNPs shows great potential and is currently the focus of intensive research.[2] This process relies on the capability of the magnetic dipole of MNPs to couple to an alternating magnetic field (AMF) and on the subsequent dissipation of the absorbed energy by its release as heat.[3] Heating using MNPs has proven to be very useful for magnetic fluid hyperthermia that promotes cell death,[4] or for controlled drug release.[5] In fact, strong thermal confinement by using the heat collectively released by MNPs has already been demonstrated to induce localized heating, which enables the activation of ion channels and neurons.[6]

Measurements of absolute temperatures of NPs have been reported using a luminescent molecular thermometer based on rare-earth-metal chelating agents.[7] Rinaldi and Polo-Corrales showed that iron oxide nanoparticles could thermally induce changes in the fluorescence of a thermoresponsive and fluorescent polymer with which the NPs were coated.[8] However, their approach is limited, as only the surpassing of one single temperature value can be detected. The assessment of local temperature increments in comparison with the global temperature of the surrounding medium, and of temperature gradients with respect to the distance from the MNP surface, has proven to be a challenging task thus far. Recently, in a remarkable study by Riedinger et al.,[9] a very accurate measurement of the surface-temperature profile of NPs was developed that is based on the thermal decomposition of a thermosensitive molecule. They were able to determine the absolute temperature at distances below 0.5 nm from the surface of the NPs.

Herein, we show that it is possible to determine the temperature, which was triggered by an AMF, in the surroundings of MNPs by the functionalization of polymer-coated MNPs with DNA (DNA-MNPs), and further hybridization with DNA that is modified with different fluorophores. Although it has already been demonstrated that magnetic[10] and gold NPs can promote DNA denaturation by thermal[11] and non-thermal processes,[12] this concept has not been used for mapping a temperature profile. By considering that double-strand DNA is one of the more rigid biological structures and that it is possible to fine-tune its melting temperature (T_m), we were able to assess an increase in local temperature by a correlation to the T_m of the DNA. Furthermore, the correlation of these local temperatures with the distance of the DNA from the surface of the MNPs allows an accurate spatial mapping of the temperature at biologically relevant distances.

We chose iron oxide NPs with a diameter of 12 nm as nanoheaters; these were obtained by following a seed-mediated growth method previously described.[13] The nanoheaters were prepared in organic solvents, and thus, a subsequent transfer to an aqueous solution was performed by means of an amphiphilic polymer shell.[14] Further details of the synthesis and characterization can be found in the Supporting Information. The amphiphilic shell provides stability and reactive points because of a high surface density of carboxylic groups for further covalent coupling with amino-modified oligonucleotides (see the Supporting Information).

The efficiency of the covalent coupling was indirectly assessed by quantifying the amount of unreacted DNA that was present in the supernatant fluids after the nanoparticles had been removed by salt precipitation. Unspecific interactions were discarded (see the Supporting Information). Moreover, the ζ-potentials of bare MNPs (-39.91 ± 0.99 mV) and DNA-MNPs (-46.22 ± 2.93 mV) corroborated the presence of DNA (molar ratio (NPs/DNA) = 1:35.95 ± 1.04), as the modification makes the ζ-potential of the conjugates nanoparticles more negative, as expected.

The measurement of the temperature of the bulk medium (global temperature) in experiments that involve inductive heating with MNPs is a routine procedure to determine the specific loss power of magnetic fluids.[15] However, to be able to fine tune this to the point where temperature in the vicinity of NPs can be measured, a strategy was required whereby a given phenomenon could be directly correlated to temperature. By incubating the DNA-MNPs with different complementary oligonucleotides with different melting temperatures, it was possible to infer temperature gradients upon AMF excitation by quantifying the denatured DNA.

DNA-MNPs were allowed to hybridize with three complementary oligonucleotides that were modified with a distinct fluorophore each. Three types of fluorophore-modified DNAs were chosen: 6-carboxyfluorescein (DNA-F), hexa-

[*] J. T. Dias, Dr. M. Moros, Dr. P. del Pino, S. Rivera, Dr. V. Grazú, Dr. J. M. de la Fuente
Instituto de Nanociencia de Aragon, Universidad de Zaragoza
C/Mariano Esquillor s/n (Spain)
E-mail: vgrazu@unizar.es
jmfuente@unizar.es
Dr. P. del Pino, Dr. J. M. de la Fuente
Fundación ARAID (Spain)

[**] We thank the ERC for the Starting Grant "NANOPUZZLE", ARAID, the Dpto de Industria Innovación (DGA), and the Fondo Social Europeo for financial support. We also thank the referees for improving the manuscript with their comments.

Supporting information for this article is available on the WWW under http://dx.doi.org/10.1002/anie.201305835.

chlorofluorescein (DNA-H), and sulforhodamine 101 acid chloride (DNA-T), which have 10, 11, and 12 base pairs (bp), respectively. These complementary strands were designed so that their 3′ end should hybridize with the first 5′ end bases of the sequence conjugated to the NPs. The total distance from the 5′ end of each hybridized DNA strand to the magnetic core of the MNPs can be assumed to be 2 nm (polymer coating) plus 3.0, 3.3, or 3.6 nm, respectively (Figure 1), because the DNA double helix possesses a rigid structure.

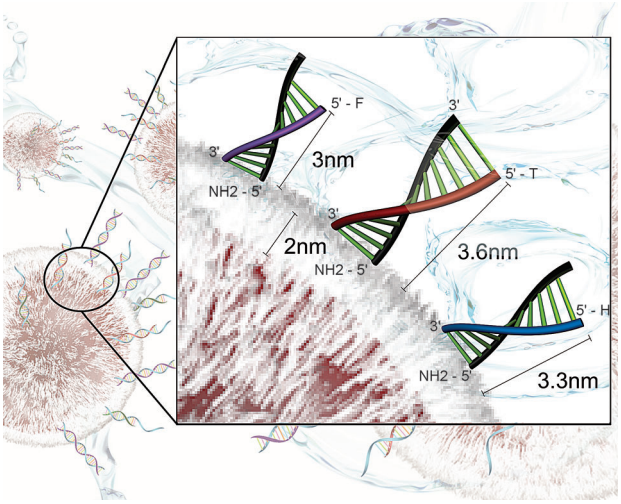

Figure 1. DNA-hybridization strategy. Three complementary oligonucleotides of different sizes (DNA-F: 10 bp, 3 nm; DNA-H: 11 bp, 3.3 nm; DNA-T: 12 bp, 3.6 nm) were designed so that their 3′ ends always hybridize with the first base of the 5′ end of the DNA strand that is covalently linked to the amphiphilic polymer (2 nm) that coats the MNPs.

A set of experiments was designed to evaluate the heating capacity of the nanoparticles under AMF (Figure 2). If we consider the NP to be a "hot" source, an increase in local temperature will denature the three DNA sequences in the AMF experiments. Samples loaded with the three distinct complementary oligonucleotides were placed in an instrument for inductive nanoheating. Each sample was subjected to seven independent experiments that were stopped when global solution temperatures of 27, 30, 33, 39, 42, and 45 °C had been reached. For all experiments, the global-temperature ramps were recorded with a temperature probe dipped into the solution (see the Supporting Information). This ramp is governed by the concentration of the sample (for all of the experiments, the Fe concentration was set to 0.42 mg mL^{-1}, which corresponds to a NP concentration of ca. 204.8 nM). The parameters selected for the inductive-nanoheating apparatus were a field amplitude of 25 kA m^{-1} and a frequency of 835.25 kHz, and the experiments were carried out with a similar global temperature ramp (ca. 0.3 °C per min). Upon removal of the AMF field, the DNA-MNPs were precipitated, and the fluorescence of the denatured complementary oligonucleotide was measured (Figure 2; for details, see the Supporting Information).

As the system used in this work implies the immobilization of the oligonucleotides onto the surface of NPs, the

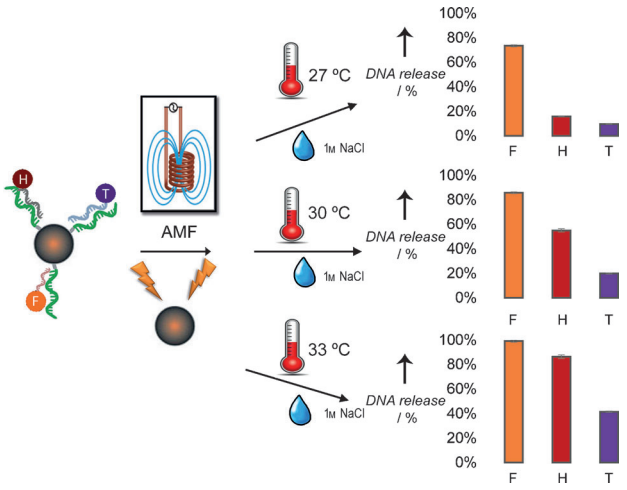

Figure 2. AMF heating of DNA-MNPs, followed by their precipitation by salt addition, and measurement of the corresponding fluorescence of the supernatants (F: DNA-F; H: DNA-H; T: DNA-T), for three of the final global temperatures reached. Release efficiencies were calculated after determination of the total DNA denatured where the samples were heated up to 95 °C for 20 min.

thermodynamics of hybridization and denaturation can differ from those expected for the same oligonucleotides in solution.[16] Therefore, the same DNA-MNPs were incubated in a thermocycler at global temperatures equivalent to those reached in the AMF experiments to correlate the amount of DNA released to the local temperature required for this release. This control experiment was set up under conditions where the global temperature is equal to the local temperature, thus DNA denaturation will solely be due to the global temperature of the apparatus.

As in the AMF experiments, the fluorescence of the denatured DNA was measured from the supernatant fluids after precipitation and centrifugation of the MNPs. Thus, it was possible to compare the amounts of DNA released in the AMF and thermocycler experiments at each global temperature reached (Figure 3 a, c, e). Furthermore, by applying the thermodynamics of DNA duplex formation, it was possible to experimentally determine the enthalpy change ($\Delta_r H$) and the entropy change ($\Delta_r S$) for each of the three oligonucleotides, and thus the temperature at which 50 % of the DNA sequences that were modified with a fluorophore will be denatured (T_m) for both the AMF and thermocycler experiments (see the Supporting Information). With a calculated T_m value and the experimental data in hand, we were able to simulate the theoretical total melting curve for each experiment with a Boltzmann sigmoidal fitting model (Figure 3 b, d, f).

The melting temperatures were approximately 10 °C lower in the AMF experiments than for the thermocycler experiments. As previously mentioned, it can be assumed that the heat in the thermocycler experiments only originates from the equipment, with no contribution from the NPs. Consequently, for AMF experiments, the local temperature in the vicinity of the NPs has to be greater than the measured global temperature.

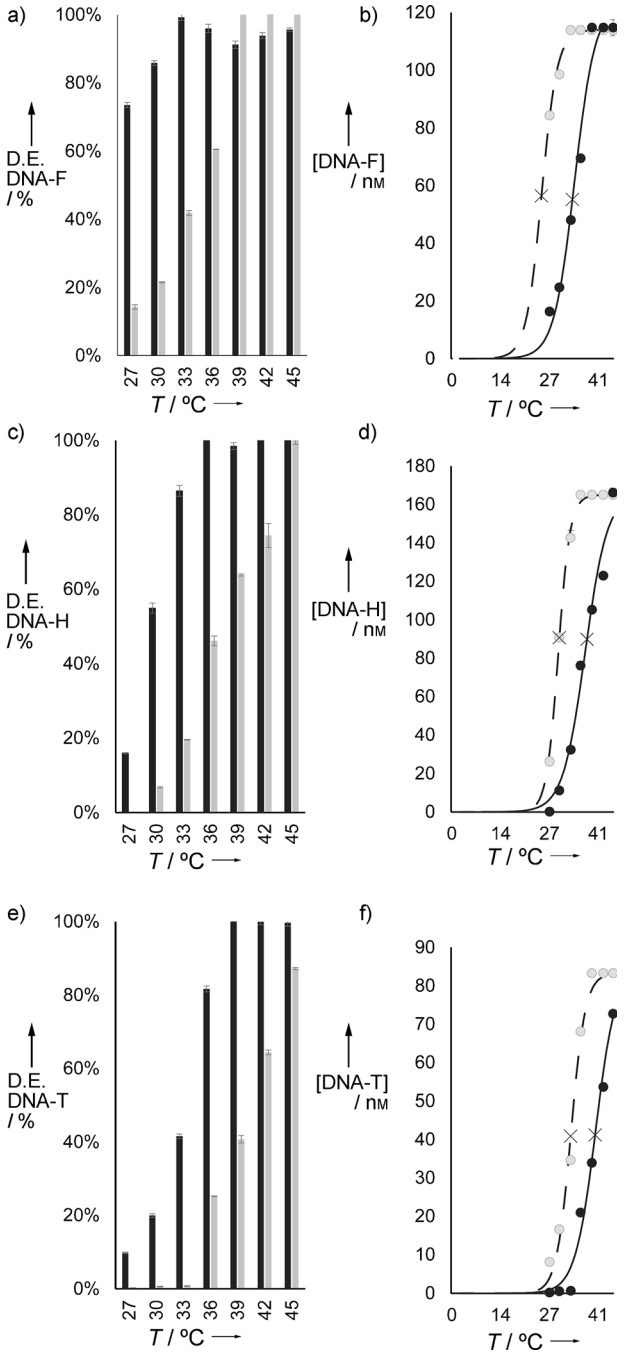

Figure 3. a), c), e) Denaturing efficiency (D.E.) in AMF (■) and thermocycler (■) experiments with the three fluorophore-modified oligonucleotides. The efficiencies were calculated by taking into account the total amount of denatured DNA when the DNA-MNPs were incubated at 95 °C for 20 min. b), d), f) Concentration of the DNA released after the AMF (●) and thermocycler (●) experiments with the three fluorophore-modified oligonucleotides, for seven global temperatures. The Boltzmann sigmoidal fitting models of the theoretical total melting curves are shown for the AMF (– – –) and thermocycler (——) experiments; they are based on the experimental points and the calculated T_m (X). Standard errors were calculated based on three independent measurements.

By interpolating the concentration of released DNA in the AMF experiments for any given global temperature onto the Boltzmann fitting model obtained from the thermocycler experiments, it was possible to simultaneously ascertain the three different local-temperature increments at the distances determined by the DNA length (5, 5.3, and 5.6 nm) from the surface of the NPs for each global temperature (Table 1 and Figure 4; see also the Supporting Information). These results demonstrate that very high temperature gradients can be found in the vicinity of NPs.

Table 1: Local temperatures determined at three different distances from the surface of the nanoparticle, and respective standard errors that were calculated based on three independent measurements.

T_G [°C]	T_L at 5 nm[a] [°C]	T_L at 5.3 nm[a] [°C]	T_L at 5.6 nm[a] [°C]
27	36.49 ± 0.10	31.99 ± 0.04	–[b]
30	38.25 ± 0.12	37.79 ± 0.17	36.14 ± 0.09
33	41.57 ± 0.38	42.87 ± 0.36	39.10 ± 0.07
36	–[b]	52.94 ± 0.62	44.16 ± 0.15
39	–[b]	–[b]	51.59 ± 0.19

[a] Distance from the nanoparticle. [b] – Measurement was not significant, as the local temperature was not enough to promote DNA denaturation from the NP surface, or the local temperature was too high and 100% of the complementary fluorescent DNA strand was denatured. T_G = global temperature, T_L = local temperature.

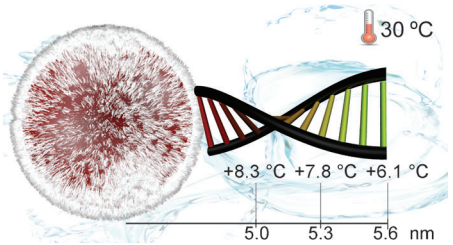

Figure 4. Temperature gradients across the DNA strands that were experimentally determined. For the example shown, T_{global} = 30 °C.

For the plasmonic excitation of Au NPs, DNA denaturation has alternatively been explained by mechanisms of hot electron injection rather than local temperature gradients.[12,17] In our case, the observed thermal confinement leads to similar conclusions as in the report of Riedinger et al. described above:[9] Classical heat-transport theory (diffusion) cannot explain these results, and a ballistic regime might be required to explain it.[9] Our results entailed an even more dramatic temperature gradient; however, this difference can be accounted for to some extent, because the system reported herein differs from that of Riedinger et al. in several key aspects. First, this work employs more concentrated solutions ([Fe] = 0.42 mg mL^{-1} vs. [Fe] = 0.02 mg mL^{-1}), and thus collective heating cannot be ruled out. Second, the oligonucleotide reporters are placed at one extreme of a hydrophobic coating of poor thermal conductivity of a length of approximately 2 nm, whereas the molecular temperature probe described by Riedinger et al. is placed at a maximum distance of 2 nm from the surface of the NPs. Third, double-stranded DNA chains are more rigid than PEG molecules and are highly negatively charged, which allows the assumption that

they extend radially from the surface of the NPs. Lastly, the MNPs in this study have a smaller diameter (12 nm vs. 15 nm), and we used harsher AMF conditions. Moreover, the molecular thermal probe presented herein represents one of the most robust systems reported until now (for more details on spatial resolution, reproducibility, and sensitivity, see the Supporting Information).

In summary, by functionalizing polymer-coated MNPs with DNA and further hybridization with DNA that was modified with different fluorophores, we were able to correlate the DNA denaturation profile and the local temperature on the NP surface. By comparing fluorescence intensities of denatured DNA after the application of an AMF and after simple global heating with a thermocycler, it was possible to verify that these MNPs act as nanoheaters during the AMF experiment. Hence, when compared with previous results, this method allows a more accurate determination of the local surface temperature of MNPs.

Received: July 5, 2013
Revised: August 16, 2013
Published online: September 23, 2013

Keywords: biofunctionalization · DNA · hyperthermia · magnetic properties · nanoparticles

[1] M. Colombo, S. Carregal-Romero, M. F. Casula, L. Gutierrez, M. P. Morales, I. B. Bohm, J. T. Heverhagen, D. Prosperi, W. J. Parak, *Chem. Soc. Rev.* **2012**, *41*, 4306 – 4334.
[2] M. Creixell, A. C. Bohórquez, M. Torres-Lugo, C. Rinaldi, *ACS Nano* **2011**, *5*, 7124 – 7129.
[3] A. Figuerola, R. Di Corato, L. Manna, T. Pellegrino, *Pharmacol. Res.* **2010**, *62*, 126 – 143.
[4] J.-H. Lee, J.-t. Jang, J.-s. Choi, S. H. Moon, S.-h. Noh, J.-w. Kim, J.-G. Kim, I.-S. Kim, K. I. Park, J. Cheon, *Nat. Nanotechnol.* **2011**, *6*, 418 – 422.
[5] M. Liong, J. Lu, M. Kovochich, T. Xia, S. G. Ruehm, A. E. Nel, F. Tamanoi, J. I. Zink, *ACS Nano* **2008**, *2*, 889 – 896.
[6] H. Huang, S. Delikanli, H. Zeng, D. M. Ferkey, A. Pralle, *Nat. Nanotechnol.* **2010**, *5*, 602 – 606.
[7] C. D. S. Brites, P. P. Lima, N. J. O. Silva, A. Millán, V. S. Amaral, F. Palacio, L. D. Carlos, *Adv. Mater.* **2010**, *22*, 4499 – 4504.
[8] L. Polo-Corrales, C. Rinaldi, *J. Appl. Phys.* **2012**, *111*, 07B334.
[9] A. Riedinger, P. Guardia, A. Curcio, M. A. Garcia, R. Cingolani, L. Manna, T. Pellegrino, *Nano Lett.* **2013**, *13*, 2399 – 2406.
[10] A. M. Derfus, G. von Maltzahn, T. J. Harris, T. Duza, K. S. Vecchio, E. Ruoslahti, S. N. Bhatia, *Adv. Mater.* **2007**, *19*, 3932 – 3936.
[11] J. Stehr, C. Hrelescu, R. Sperling, G. Raschke, M. Wunderlich, A. Nichtl, D. Heindl, K. Kürzinger, W. Parak, T. Klar, J. Feldmann, *Nano Lett.* **2008**, *8*, 619 – 623.
[12] R. Huschka, J. Zuloaga, M. Knight, L. Brown, P. Nordlander, N. Halas, *J. Am. Chem. Soc.* **2011**, *133*, 12247 – 12255.
[13] S. Sun, H. Zeng, D. B. Robinson, S. Raoux, P. M. Rice, S. X. Wang, G. Li, *J. Am. Chem. Soc.* **2004**, *126*, 273 – 279.
[14] M. Moros, B. Pelaz, P. Lopez-Larrubia, M. L. Garcia-Martin, V. Grazu, J. M. de La Fuente, *Nanoscale* **2010**, *2*, 1746 – 1755.
[15] J.-P. Fortin, C. Wilhelm, J. Servais, C. Ménager, J.-C. Bacri, F. Gazeau, *J. Am. Chem. Soc.* **2007**, *129*, 2628 – 2635.
[16] D. Mocanu, A. Kolesnychenko, S. Aarts, A. T. Dejong, A. Pierik, W. Coene, E. Vossenaar, H. Stapert, *Anal. Biochem.* **2008**, *380*, 84 – 90.
[17] B. Aoune, H. Ryan, B. Rizia, W. K. Mark, J. H. Naomi, *Chem. Phys. Lett.* **2009**, *482*, 171 – 179.

